

# An Improved Data Privacy Diagnostic Framework for Multiple Machinery Components Data Based on Swarm Learning Algorithm

Shilong Sun<sup>ID</sup>, Member, IEEE, Haodong Huang<sup>ID</sup>, Tengyi Peng<sup>ID</sup>, and Dong Wang<sup>ID</sup>, Member, IEEE

**Abstract**—The continuous operation of the equipment degrades the performance of the critical parts, which can cause the equipment to fail and stop at a particular and unexpected moment. Timely diagnosis of the equipment is vital for condition monitoring and maintenance. Due to the small amount of data and data collection limitation, it is difficult to train an efficient diagnosis model for real-time tracking within only one piece of equipment data. This study proposes an improved data privacy diagnostic framework for multiple same types of machinery components, solving the insufficient data, data protection, and multiple machines' fault information exchange. First, the swarm learning (SL) framework integrates various data sources to enrich the data contained within a solo diagnosis network. Second, the different training nodes utilize various local diagnosis models to improve data protection efficiency further and realize the interaction of data information. Third, we developed three different local diagnosis models, which can mutually exchange the partially faulty information with each other to make up for the inefficiency of model diagnosis caused by single insufficient data. The experimental demonstration is conducted on the bearing fault datasets, proving that the proposed method can be more flexible and reliable in more industrial scenarios.

**Index Terms**—Data privacy protection, different local diagnosis model, global fault diagnosis, multiple machinery components, swarm learning (SL).

## I. INTRODUCTION

**F**AULT diagnosis technology is of great significance in modern industrial systems. Timely detection of faults in the system can improve the safety and reliability of complex systems. By identifying the causes of faults, appropriate measures can be taken to rectify the system failures [1], [2]. One effective approach involves the placement of sensors along

Manuscript received 27 June 2023; revised 11 August 2023; accepted 17 August 2023. Date of publication 30 August 2023; date of current version 15 September 2023. This work was supported in part by the Natural Science Foundation of Guangdong Province under Grant 2021A1515110615 and in part by the National Natural Science Foundation of China under Grant 51975355. The Associate Editor coordinating the review process was Dr. Ke Feng. (*Corresponding author: Shilong Sun*)

Shilong Sun, Haodong Huang, and Tengyi Peng are with the School of Mechanical Engineering and Automation and the Guangdong Provincial Key Laboratory of Intelligent Morphing Mechanisms and Adaptive Robotics, Harbin Institute of Technology, Shenzhen 518055, China (e-mail: sunshilong@hit.edu.cn; hhd1340201839@163.com; 20s053007@stu.hit.edu.cn).

Dong Wang is with the State Key Laboratory of Mechanical System and Vibration, Shanghai Jiao Tong University, Shanghai 200240, China (e-mail: dongwang4-c@sjtu.edu.cn).

Digital Object Identifier 10.1109/TIM.2023.3310057

the horizontal and loading directions of the force-bearing components of rotating equipment. This arrangement allows for real-time monitoring of equipment operation and enables subsequent prediction work. The abundance of data has fueled the rapid development of data-driven fault diagnosis methods [3], [4], [5].

With the introduction of deep learning, fault diagnosis has been further developed due to its short training time and fast convergence advantages. Some typical neural networks have been widely used, e.g., convolutional neural networks (CNNs) [6] and deep belief networks (DBNs) [7]. Peng et al. [8] proposed a Bootstrap Your Own Latent (BYOL) network based on contrastive learning algorithm automatic fault feature extractor (AFFE), which can automatically extract fault features without label information. At the same time, this study introduces data enhancement, which can help AFFE extract features from unlabeled bearing fault data. Wang et al. [9] proposed a fully interpretable network to realize machine state monitoring, which introduces interpretable statistics: warpage, negative entropy, Gini index, and smoothing factor to replace the extreme learning machine (ELM) neurons, and not only improves the interpretability of the network making it industrially usable but also reduces the parameters to improve the speed of network training. Michau et al. [10] proposed a fully unsupervised deep learning framework capable of extracting meaningful sparse representations of raw high-frequency signals. In this work, the denoising fast discrete wavelet transform is embedded in the system without any form of preprocessing and postprocessing. Zhang et al. [11] proposed a new interpretable fault diagnosis method, which extracts the features of the data through CNN, then uses principal component analysis (PCA) to reduce the dimensionality of the data, selects the first two principal components after dimensionality reduction as the fault feature vectors, and finally uses fuzzy mean clustering to realize the classification of fault feature vectors. These fault diagnosis methods based on deep learning rely on huge training data, but in the actual industry, there may be problems with a small amount of data and unknown parts of data labels. At the same time, the practical application of deep learning is limited due to the uninterpretable nature of the trained model.

However, in actual industrial settings, labeled condition monitoring data are often collected, and developing a high-precision data-driven fault diagnosis model for a single factory

can be economically and time-consuming [12], [13], [14]; federated learning (FL) technology has gained widespread adoption and can be used to address this challenge. It allows for resolving “data islands” where data are not interoperable. Furthermore, each enterprise places a high value on virtual property, making sharing data among various production plants challenging. FL provides a solution by allowing data to be trained locally while only sharing the gradient or the trained model.

In addition to addressing issues such as insufficient data and data privacy protection, the introduction of FL can also tackle challenges such as data class imbalance, non-independent and nonidentically distributed data from different sources, and model aggregation methods in industrial applications [15]. For example, Lu et al. [16] proposed a distributed wind turbine fault diagnosis FL framework class-imbalanced privacy-preserving FL (CI-PPFL) in response to industrial big data privacy protection and wind turbine data. At the same time, different servers have different amounts of data, and a noise gradient mechanism is added to prevent client gradient tracking. Zhang et al. [17] proposed a new dynamic verification scheme under the framework of FL to reduce the impact of distributed low-quality training data. During training, a verification set is added to evaluate the model, the cross-entropy loss measure is calculated, and the local model score is obtained. The model with the highest score is automatically ignored. Liu et al. [18] proposed an asynchronous FL algorithm to solve the data island problem of photovoltaic power plants. Compared with a single photovoltaic power station, multiple photovoltaic power stations can provide enough fault samples, and asynchrony can solve the problem of the different computing power of each photovoltaic power station server. Zhang et al. [19] designed an adaptive method to adjust the model aggregation interval according to the user’s feedback to reduce the communication cost while ensuring the accuracy of the model. The methods proposed above are all applications of FL in fault diagnosis of mechanical equipment, which solve the problem of insufficient data and feature distribution in different fields. Nevertheless, FL has the problem of high communication costs.

The fault diagnosis network based on FL requires a traditional central cluster server to collect and distribute information [20]. In contrast, swarm learning (SL) does not require such a central server. It can designate any node within a local area network as a temporary virtual central server to handle command issuance and collection. SL can significantly reduce communication time and computational costs. Sun et al. [21] researched an SL computational framework based on data privacy protection. In this framework, each local network node has the same fault diagnosis model, which does not align with the different data distributions in each device or factory in reality. Therefore, we improved the framework to enable each node to independently perform local fault diagnosis tailored to its unique data structure distribution. We then designed weight parameter average algorithms to facilitate the transfer of features between different local diagnostic models, enabling feature sharing while keeping the data retained locally.

Both FL and SL have their own advantages, such as data privacy protection, leveraging the capabilities of edge computing devices, only transmitting model parameters, and real-time model updates. However, due to the “one-to-many” and “many-to-one” architecture characteristics of FL, it is susceptible to attacks. Moreover, FL’s reliance on a central server can lead to issues of power concentration and also increase the cost of gradient transmission. In contrast, SL employs a point-to-point connection approach, making the architecture more stable. Each node has the potential to become a central server, which can reduce data communication costs to some extent. In the domain of fault diagnosis, FL offers a promising solution with its emphasis on data privacy and secure model aggregation. In fault diagnosis applications, where equipment condition data might be sensitive, FL enables various stakeholders to collaboratively train a fault detection model without sharing raw data. This ensures the confidentiality of sensitive information while benefiting from a diverse range of data sources. The decentralized approach also allows localized training on distributed devices, which is especially valuable for real-time monitoring of equipment health. However, the communication overhead between the central server and devices, as well as the potential challenges stemming from device heterogeneity, should be considered while implementing FL for fault diagnosis tasks. SL, on the other hand, introduces a novel dimension to fault diagnosis by leveraging collaborative knowledge exchange among nodes. In the context of fault diagnosis, where multiple equipment might exhibit diverse failure modes, SL allows nodes to share insights and partial fault information. This leads to a collective intelligence that enhances the fault diagnosis accuracy by pooling the collective expertise of different devices. SL’s adaptability to varying fault patterns and its fault tolerance capabilities make it a compelling solution for scenarios where fault diagnosis accuracy relies on the collective insights of multiple sources. Nonetheless, the complexity of swarm communication and potential resource consumption must be carefully managed to harness its full potential in fault diagnosis applications. Fig. 1 shows the comparison of FL and SL network structure.

To address the data silos and privacy protection, we employ SL as a framework for aggregating data information. In addition, each node utilizes a distinct model to enhance data privacy and improve the usability of the vibration strength model framework. The research focuses on vibration signals, such as bearings. The main innovations and creativities of this study are given as follows.

- 1) Proposing the concept of global diagnosis, where different diagnosis models can be selected randomly for various fault signals. This approach enables the optimization of diagnosis accuracy within a single network.
- 2) Designing a swarming learning structure with three local nodes as the core network for integrating data information and a virtual center to address data privacy protection concerns.
- 3) Developing different local diagnosis models for each node, comprising AlexNet, AlexNet with wavelet transformation, and AlexNet with Chebyshev filter. These models contribute to the overall fault diagnosis process.

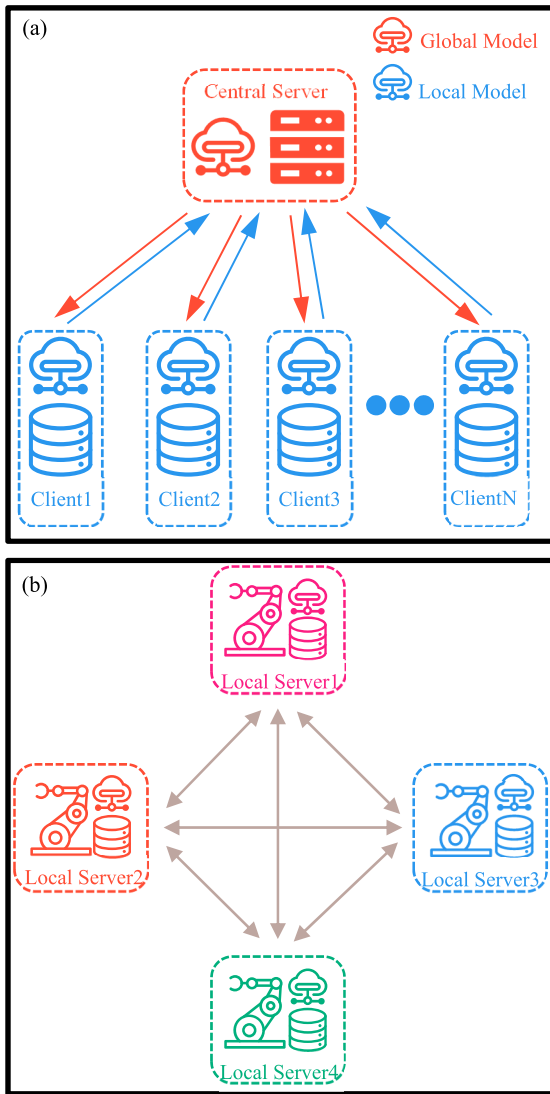


Fig. 1. Conceptual diagram of the structures of two methods. (a) FL: data are stored in individual member nodes, with a central server responsible for integrating information from each node and distributing the model. (b) SL: this method does not rely on a central server.

Three main contributions can be summarized in this study: data privacy protection, data insufficiency supplementation, and fault information exchange.

#### A. Data Privacy Protection

The study addresses the issue of data privacy protection by utilizing SL, which allows data to be locally retained while enabling the sharing of relevant information among nodes. This approach enhances the privacy and security of sensitive data.

#### B. Data Insufficiency Supplementation

The research tackles the problem of insufficient data by employing an SL framework. Each node utilizes a different model, allowing for the integration of diverse data sources and enhancing fault diagnosis's overall accuracy and reliability.

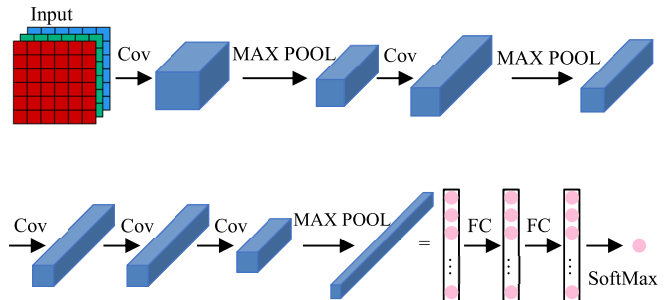


Fig. 2. AlexNet structure diagram.

#### C. Fault Information Exchange

The study focuses on facilitating the exchange of fault-related information among nodes. By employing SL, the framework enables sharing features between local diagnostic models. This promotes effective collaboration and improves fault diagnosis algorithms, enhancing diagnostic efficiency.

The remainder of this article is organized as follows. Section II briefly introduces related work such as AlexNet and SL. Section III describes the proposed method's detailed process, including each node's local training model structure and the process of SL aggregation model parameters. Section IV uses different experimental vibration signals for verification. Section V draws the conclusions.

## II. RELATED WORK

#### A. AlexNet

AlexNet [22] is a kind of CNN born in 2012. Compared with the simplest LeNet5, it has a more complex structure and more parameters for training. The overall network structure of AlexNet includes one input layer, five convolutional layers, two fully connected layers, and one output layer. The network structure of AlexNet is shown in Fig. 2.

Since the signal based on the rolling bearing is a 1-D signal, 1-D AlexNet is used to extract features from the vibration data. The calculation formula of the convolutional layer is given as follows:

$$X_j^l = f \left( \sum_{i \in M_j} X_i^{l-1} * K_{ij}^l + b_j^l \right). \quad (1)$$

Among them,  $M_j$  is the selected input feature,  $X_i^{l-1}$  is the  $j$ th input of layer  $l$ ,  $*$  is the convolution operation,  $K_{ij}^l$  and  $b_j^l$  are the weight and bias, respectively, and  $f$  is the activation function in the convolution operation. After the convolutional layer, the features can be obtained, so the pooling layer is used for downsampling to reduce model parameters and retain the main features. The calculation formula of the pooling operation is

$$y_j^l = f(\beta^{l+1} \text{down}(X_j^l) + b^{l+1}). \quad (2)$$

Among them,  $\text{down}(\cdot)$  is the downsampling operation and the pooling type. If it is  $2 \times 2$ , then its value is 0.25.

In the AlexNet structure, since there is no division operation in ReLU, it is widely used. At the end of the network operation, SoftMax is used to achieve the classification to predict

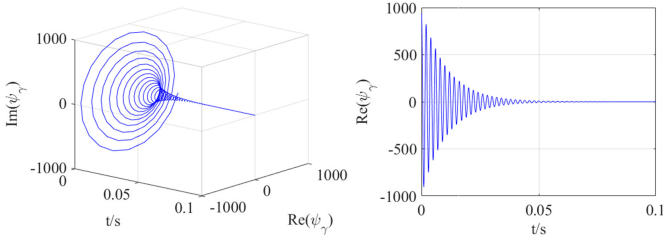


Fig. 3. Laplace wavelet waveform.

the probability of different categories, and cross entropy is used as the loss function of model training.

The choice of AlexNet as the local diagnostic model in this study is due to its excellent performance in image classification and deep learning capabilities, as well as its computational efficiency. Furthermore, its compatibility with the SL framework enables efficient information sharing and collaboration among nodes. These features contribute to enhancing the efficiency and accuracy of equipment condition monitoring.

#### B. Wavelet Network

Wavelet has attenuation and volatility. Compared with the Fourier transform, the wavelet transform is a localized time and frequency analysis. It gradually refines the signal (function) on multiple scales through scaling and translation operations and finally achieves time fineness at high frequencies. Subdivision, frequency subdivision at low frequency can automatically adapt to the requirements of time–frequency signal analysis. Wavelets can be expressed as

$$WT(a, \tau) = \frac{1}{\sqrt{a}} \int_{-\infty}^{\infty} x(t) \psi^* \left( \frac{t - \tau}{a} \right) dt. \quad (3)$$

It can be seen from the formula that the Fourier transform of different domains of wavelet has only one variable of frequency, and the wavelet has two variables: scale factor  $a$  and translation factor  $\tau$ .  $\psi^*(\cdot)$  is the complex conjugate of the generating function. By transforming (3), we can get

$$WT(a, \tau) = \frac{1}{\sqrt{a}} F^{-1} \{ X(f) \psi^*(af) \}. \quad (4)$$

From (4), it can be concluded that the wavelet transform of the signal can be regarded as the signal passing through a bandpass filter.

Li et al. [23] used the wavelet as the first layer of CNN to conduct comparative experiments and found that the Laplace wavelet can better extract the impact part due to its decreasing spiral characteristics. It can be expressed as

$$\begin{aligned} \psi(\omega, \zeta, \tau, t) &= \psi_\gamma(t) \\ &= \begin{cases} Ae^{-\frac{\zeta}{\sqrt{1-\zeta^2}}\omega(t-\tau)} e^{-j\omega(t-\tau)}, & t \in [\tau, \tau + W] \\ 0, & \text{other.} \end{cases} \end{aligned} \quad (5)$$

Among them,  $\gamma = \langle \omega, \zeta, \tau \rangle$  represents the parameters of the Laplace wavelet and  $\omega$  represents the frequency, which determines the oscillation frequency of the Laplace wavelet; the damping ratio  $\zeta$  makes the Laplace wavelet attenuate

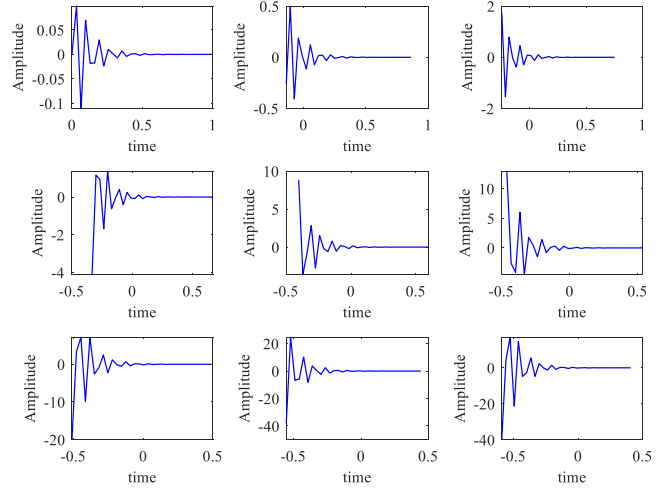


Fig. 4. Generated Laplace wavelet waveform.

rapidly,  $\tau$  is the time parameter,  $A$  is used to normalize the wavelet function, and  $W$  represents the wavelet compact support interval width. The diagram of Laplace wavelet is shown in Fig. 3.

Subsequently, the Laplace wavelet is used as the first layer of AlexNet. Since the first layer of AlexNet involved in this study originally had 64 convolution kernels, 64 Laplace wavelets need to be generated to replace the previous 64 convolution kernels. The generated multiple Laplace wavelet waveforms are shown in Fig. 4.

#### C. Filter Network

The Chebyshev filter is a filter whose frequency response amplitude is equiripple in the passband or stopband, and the amplitude characteristic is equiripple in the passband. Chebyshev type I filters are characterized by equal ripples in the passband, monotonic in the stopband, and a faster drop in the stopband. The relationship between the magnitude and frequency of the  $n$ -order Chebyshev type I filter is given as follows:

$$G_n(\omega) = |H_n(j\omega)| = \frac{1}{\sqrt{1 + \varepsilon^2 T_n^2 \left( \frac{\omega}{\omega_0} \right)}}. \quad (6)$$

Among them,  $\varepsilon < 1$ , which is related to the ripple of the passband, the larger the value, the bigger the ripple.  $n$  is the order of the filter, and  $T_n(\omega/\omega_0)$  is the Chebyshev polynomial.

As mentioned above, the filter must replace the convolution kernel of the first layer of AlexNet, so 64 Chebyshev filters must be generated.

#### D. Swarm Learning

Fig. 1(b) shows a schematic of the diagnostic structure based on the SL network. The SL network authorizes each participant (local client) to share and update the model, which means that each participant has the same capabilities as the FL central server. Therefore, each participant can integrate information from multiple other edge computing node participants. Each participant should complete two steps during the training

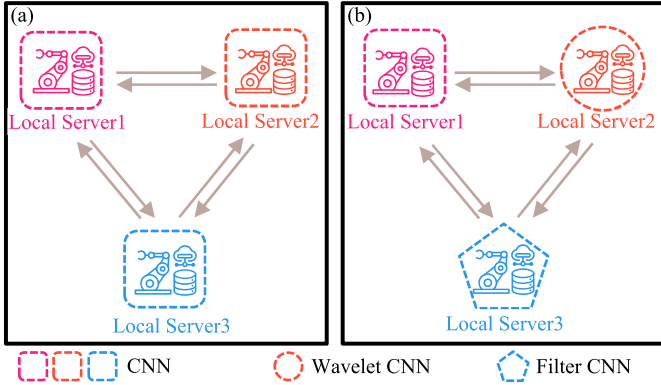


Fig. 5. Comparison of (a) SL framework and (b) DSL framework.

process to ensure the model's accuracy. First, each node first trains the model locally. After each epoch, one of the nodes is randomly selected as the node for integrating the model. After the model is integrated, the model is distributed to other nodes until the end of the epoch is reached. Model integration adopts the method of averaging model parameters, and the calculation formula is given as follows:

$$\mathbf{m}_{j+1} = \frac{1}{n} \sum_{i=1}^n \mathbf{m}_{j,i}. \quad (7)$$

In the formula,  $\mathbf{m}_{j+1}$  is the integrated model parameter,  $i$  is the number of nodes, and  $\mathbf{m}_{j,i}$  is the model parameter obtained by the node after the  $j$ th round of training.

### III. PROCEDURE OF THE PROPOSED METHOD

Sun et al. [21] proposed the use of SL as a framework for fault diagnosis. This framework utilizes the same CNN to train the local model. However, we propose using different algorithms to train the local diagnosis model in this study. This concept aims to make the specific signal choose the specific diagnosis model and also make them exchange their fault information rather than the original dataset. It can be used in three practical industrial scenarios: data insufficient, fault information exchange, and privacy protection. After each training epoch, the model parameters are summed, averaged, and distributed to each node. Domain adaptation neural network (DANN) is also introduced to reduce the distribution difference of data between various domains [21]. The comparison between the SL and the different model swarm learning models is shown in Fig. 5.

The proposed method can automatically learn fault features from fault data and identify machine working status from raw vibration signals. The overall process of the proposed mechanical fault diagnosis process is shown in Fig. 6. See Algorithm 1 for the training algorithm.

### IV. EXPERIMENTAL RESULTS AND COMPARISONS

This section uses the different bearing datasets to verify our assumption and global diagnosis framework. We design four experiments to evaluate the performance and effectiveness of our proposed different swarm learning (DSL) framework.

---

#### Algorithm 1 Fault Diagnosis of Different Models

---

##### I. Data preprocessing

##### II. Model preparation

1) Select AlexNet as the skeleton of the model and the model of one of the nodes

2) Replace the first layer of AlexNet with Laplace wavelet and Chebyshev filter, respectively as the model of the other two nodes

##### III. Build a DSL framework

##### IV. Model training

1) For any node,  $i = 1, 2, 3$ ;

Choose one of the three nodes as the model decision-maker  $m_{j,k_{th}} = (\omega_{k_{th}} | b_{k_{th}})$ ;

2) Model parameter update and distribution

##### V. Model validation

---

TABLE I  
WORKING CONDITIONS OF THREE BEARING FAULT DATASETS

Data Set	Load	Speed(rpm)	Fault diameter	Sampling frequency (Hz)
CWRU	1HP	1772	7 miles	12k
HITsz	1kN	1200	0.3mm	25.6k
SCU	1kN	896.1	0.3mm	10k

#### A. Dataset Preparation

The research object in the experiment is three nodes, and the datasets of the three nodes come from different sources, namely, Kate Western Reserve University dataset (CWRU), Soochow University dataset (SCU), and laboratory self-made dataset (HITsz). The details of the bearing fault test bench are shown in Fig. 7.

- 1) *Dataset A (SCU)*: The dataset of the fourth node comes from the Soochow University dataset.
- 2) *Dataset B (HITsz)*: The dataset for the second node is obtained from our own laboratory collection.
- 3) *Dataset C (CRWU) [24]*: The dataset of the first node is the public dataset of Case Western Reserve University.

There are four types of bearing status: normal, inner ring fault, outer ring fault, and rolling element fault. Since the research problem is a small sample, the dataset of each node has 404 sets of data, and the length of each set of data is 1200. For each node, 200 are used for training and 204 are used for testing. For each type of fault, 50 sets of data are used to train the diagnostic model, while 51 sets of data are used to test the model. The working conditions of each dataset are listed in Table I.

#### B. Hyperparameter Settings

The fault diagnosis of different models based on the DSL framework is implemented using the Python-based Pytorch framework. The epoch is set to 100, as referred to in [21]. Through experimental fine-tuning, it has been observed that when the epoch is greater than 100, the loss function remains essentially unchanged. The learning rate is set to 0.0003, which is adapted and fine-tuned from the learning rate of SL

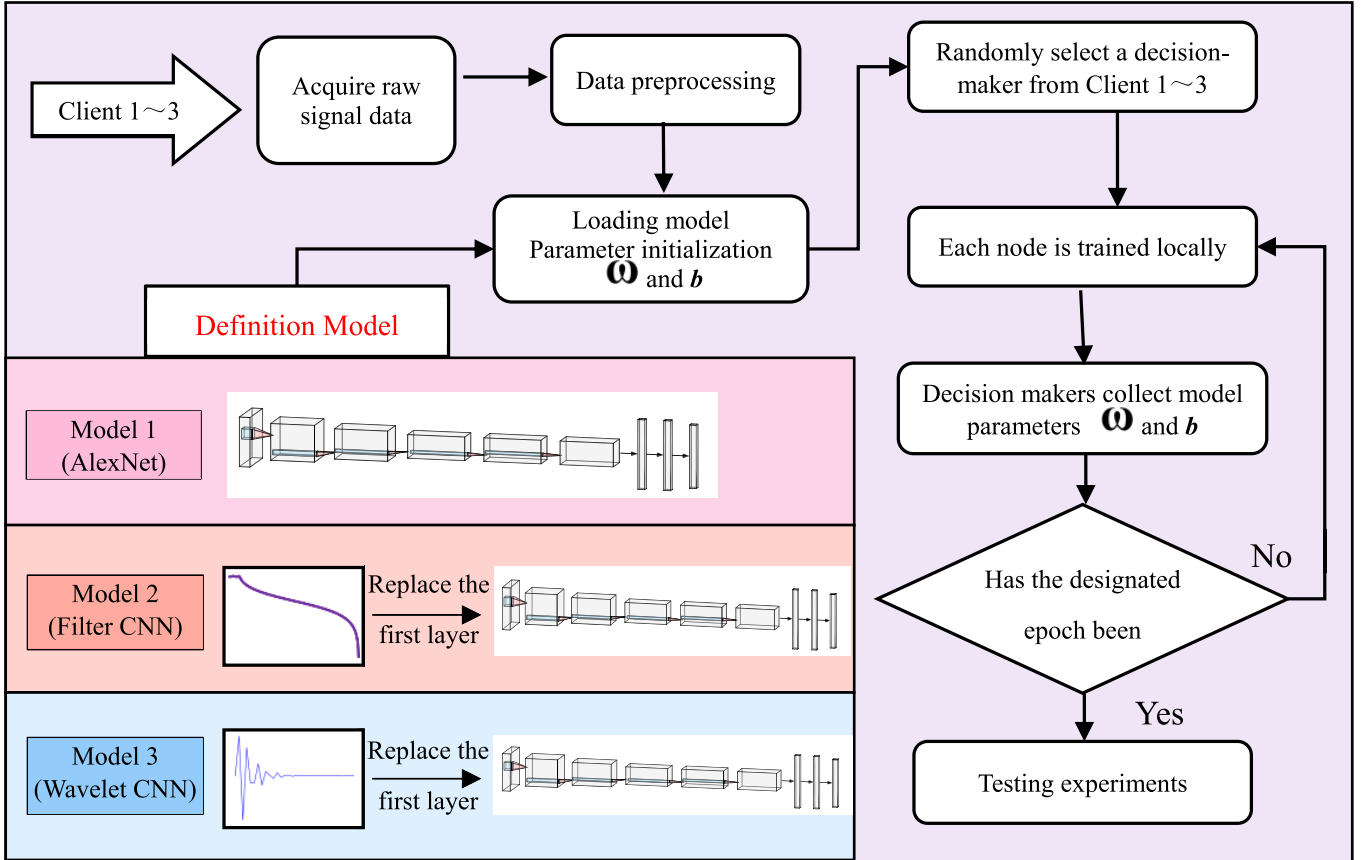


Fig. 6. Flowchart of fault diagnosis based on the proposed method.

TABLE II  
HYPERPARAMETER SETTINGS

Parameter	Value
epoch	100
learning rate	0.0003
$N_{train}$	50
batch size	16
$N_{test}$	51

in [21]. The sizes of the training set ( $N_{train}$ ) and the test set ( $N_{test}$ ) follow the conventions laid out in [8].

The hyperparameter settings for the experiments are listed in Table II.

### C. Experiment Settings

The abovementioned experimental parameter setting experiment was run five times in total, and the algorithm took 64 s to run each time. The experimental results are shown in Table III.

It is not difficult to find from Table IV that good accuracy can be obtained in repeated experiments, which shows the feasibility of the experiment. At the same time, the running time is short, and faults can be found in time in actual industrial applications.

### D. Computational Cost Comparison

In this section, we discussed three primary learning methods: FL, SL, and swarm learning with different models. For

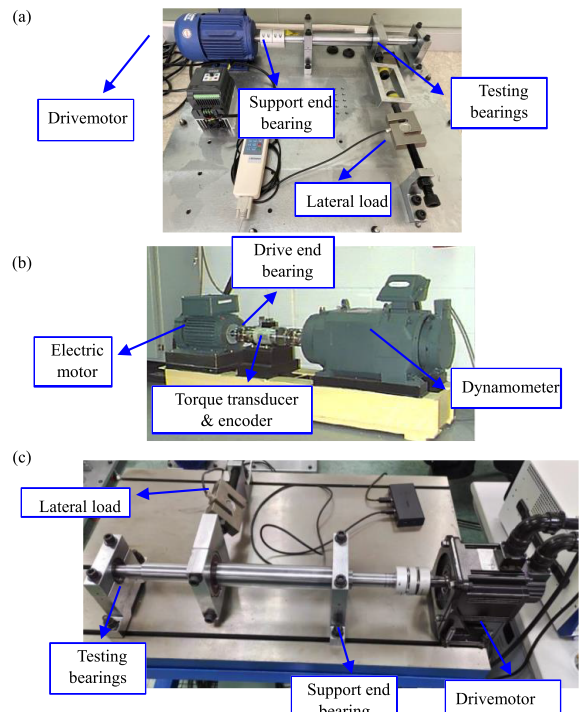


Fig. 7. Bearing fault test rig: (a) SCU, (b) CWRU, and (c) HITsz.

each method, we evaluate it from two main perspectives: the number of model parameters and data transfer times.

TABLE III  
EXPERIMENTAL RESULTS OF RUNNING FIVE TIMES

Number of nodes\AC C	1	2	3	4	5	Average\Standard Deviation
Node 1	0.99 5	0.99	1	1	1	0.997±0.004
Node 2	0.98 5	0.99	0.97 5	0.9 1	0.98 8	0.9832±0.0078
Node 3	1 5	0.99	0.99 5	1	1	0.998±0.0024

TABLE IV  
COMPARISON OF COMPUTATIONAL COST

	Number of parameters	Data transfer times
FL[25]	10679796	6/epoch
SL[21]	10679796	4/epoch
DSL	10679628	4/epoch

From Table IV, we can observe that the DSL has fewer parameters compared to FL and SL, and for the data transfer times, it has four times for each epoch, while the FL has six times for each epoch. The reason is that SL and DSL do not need a central server, while FL needs a central server, which needs two more times of data transfer: uploading and downloading data. These uploading and downloading require more data transfer time. This computation cost can be significant when the dataset becomes a large-scale one.

#### E. Comparative Experiment

To further study the feasibility of the proposed DSL, this section sets up multiple experiments and different situations to verify.

1) *Experiment I (Compared With SL)*: This experiment studies the influence of different models on the experimental results. In [21], some identical CNN models are used, so this experiment is set up for comparison. During the experiment, except that the wavelet CNN and filter CNN in DSL were replaced by AlexNet, other experimental parameters and network structure remained unchanged. The experimental results are shown in Fig. 8.

The experimental results show that both DSL and SL methods have achieved good results, but DSL has higher accuracy in comparison. This indicates that the difference of the model not only does not hinder the communication of the model, but the accuracy is also further improved. At the same time, the introduction of wavelet and filter enables the network to extract the impact characteristics of the fault better than the ordinary 1-D CNN and gives the network a certain interpretability.

2) *Experiment II (Comparison With Local Learning)*: This experiment is to compare DSL with local learning. The experiment is divided into two parts. One part is the method of DSL proposed in this article. One part is local training, that

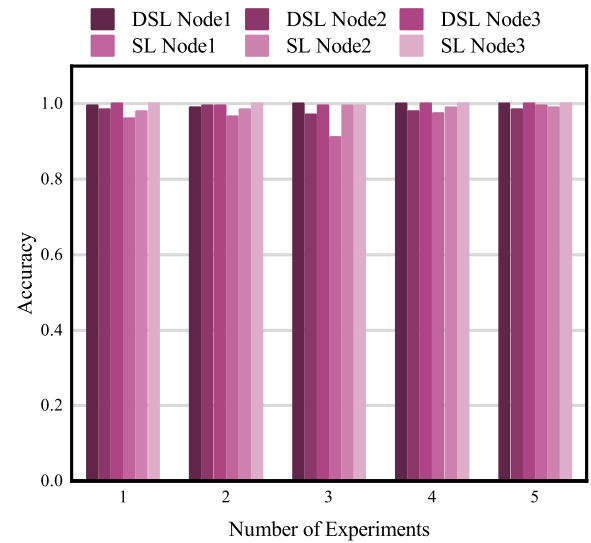


Fig. 8. Comparison of experimental results of SL and DSL.

TABLE V  
COMPARISON BETWEEN DSL AND LOCAL LEARNING

Accuracy	DSL	Local learning
Node 1	0.99	1
Node 2	0.995	0.961
Node 3	0.995	1

is, there is no model interaction process between the three nodes, and both training and testing are performed locally. The experimental results are shown in Table V.

Table V shows the experimental results of DSL and local learning. If network parameters are not integrated and only local training is conducted, excellent results can be obtained due to the same data sources. However, in comparison, the results under the DSL framework are very close to local learning, and the accuracy is slightly higher on node 2.

3) *Experiment III (Dataset Size on Experimental Results)*: This experiment studies the influence of the size of the training set on fault diagnosis under the DSL framework. This experiment selects the vibration signal as the time-domain signal. Since the batch size is 16, the size of the dataset is set to 16, 40, 80, 100, 120, 160, and 200. The experimental results are shown in Fig. 9.

From the experimental results, it can be concluded that the experiment's accuracy increases with the training set's size. When the dataset is small, that is, when there are only four data of each type for each node, the experimental accuracy is poor. However, as the number increases to 10, the accuracy rapidly increases, indicating that the proposed DSL framework can run on a smaller training set size but is also relatively weak when the data are extremely scarce.

4) *Experiment IV (Data Category Imbalance)*: In the above experiment, the dataset of each node is the same, and the data for each type of fault are the same. This experiment aims to explore the impact of missing class data on the experimental results. The experimental setup is given as follows: Node 1 is missing outer circle fault data, Node 2 is the missing rolling

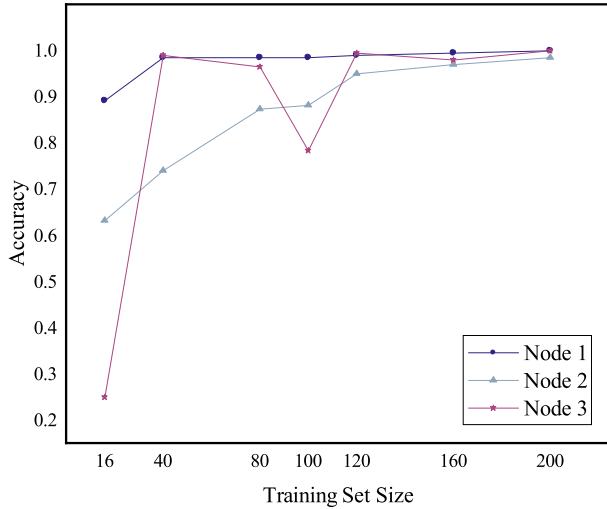


Fig. 9. Accuracy of different training set sizes under DSL.

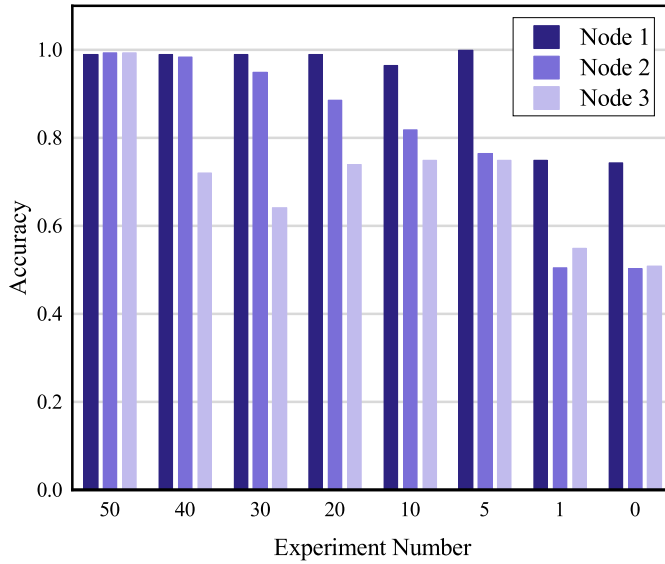


Fig. 10. Experimental results with missing training data. Different colors represent different nodes, and each node lacks different data types.

element fault data, Node 3 is the missing inner circle fault data, and each node has normal data. In the above experiment, the fault data for each type of node are 50, which is now adjusted to 40, 30, 20, 10, 5, 1, and 0. The experimental results are shown in Fig. 10. In this experiment, the data of each node are unbalanced. The experimental results indicate that in the DSL framework, data loss significantly impacts the experimental results. When less data are missing, the accuracy of Nodes 1 and 2 slightly decreases, while the accuracy of Node 3 substantially decreases. When the data are highly missing, the accuracy of each node is not high.

## V. CONCLUSION

This article presents a fault diagnosis algorithm for different models based on the DSL framework. This diagnostic framework can protect data privacy, has a shorter training time, and contains various local diagnostic models, making the proper signal match the suitable diagnosis models. This study

proposes an improved data privacy diagnostic framework based on an SL algorithm to realize fast and accurate diagnosis, especially for multiple machines. First, the SL framework integrates various data sources to enrich the data contained within a solo diagnosis network. Second, the different training nodes utilize various local diagnosis models to improve data protection efficiency further and realize the interaction of data information. Third, we develop three different local diagnosis models, which can mutually exchange the partially faulty information with each other to make up for the inefficiency of model diagnosis caused by single insufficient data. The feasibility of the proposed method is verified by setting up a series of comparative experiments based on different bearing fault signals. Therefore, this proposed conceptual global diagnosis model can be applied to broader industrial application scenarios requiring data privacy protection and fault diagnosis.

## REFERENCES

- [1] C. Li, S. Zhang, Y. Qin, and E. Estupinan, "A systematic review of deep transfer learning for machinery fault diagnosis," *Neurocomputing*, vol. 407, pp. 121–135, Sep. 2020.
- [2] H. Shao et al., "Fault diagnosis of a rotor-bearing system under variable rotating speeds using two-stage parameter transfer and infrared thermal images," *IEEE Trans. Instrum. Meas.*, vol. 70, 2021, Art. no. 3524711.
- [3] X. Li, W. Zhang, N.-X. Xu, and Q. Ding, "Deep learning-based machinery fault diagnostics with domain adaptation across sensors at different places," *IEEE Trans. Ind. Electron.*, vol. 67, no. 8, pp. 6785–6794, Aug. 2020.
- [4] H. Wang, S. Li, L. Song, L. Cui, and P. Wang, "An enhanced intelligent diagnosis method based on multi-sensor image fusion via improved deep learning network," *IEEE Trans. Instrum. Meas.*, vol. 69, no. 6, pp. 2648–2657, Jun. 2020.
- [5] J. Zhang, Y. Sun, L. Guo, H. Gao, X. Hong, and H. Song, "A new bearing fault diagnosis method based on modified convolutional neural networks," *Chin. J. Aeronaut.*, vol. 33, no. 2, pp. 439–447, Feb. 2020.
- [6] F. Jia, Y. Lei, N. Lu, and S. Xing, "Deep normalized convolutional neural network for imbalanced fault classification of machinery and its understanding via visualization," *Mech. Syst. Signal Process.*, vol. 110, pp. 349–367, Sep. 2018.
- [7] H. Shao, H. Jiang, H. Zhang, and T. Liang, "Electric locomotive bearing fault diagnosis using a novel convolutional deep belief network," *IEEE Trans. Ind. Electron.*, vol. 65, no. 3, pp. 2727–2736, Mar. 2018.
- [8] T. Peng, C. Shen, S. Sun, and D. Wang, "Fault feature extractor based on bootstrap your own latent and data augmentation algorithm for unlabeled vibration signals," *IEEE Trans. Ind. Electron.*, vol. 69, no. 9, pp. 9547–9555, Sep. 2022.
- [9] D. Wang, Y. Chen, C. Shen, J. Zhong, Z. Peng, and C. Li, "Fully interpretable neural network for locating resonance frequency bands for machine condition monitoring," *Mech. Syst. Signal Process.*, vol. 168, Apr. 2022, Art. no. 108673.
- [10] G. Michau, G. Frusque, and O. Fink, "Fully learnable deep wavelet transform for unsupervised monitoring of high-frequency time series," *Proc. Nat. Acad. Sci. USA*, vol. 119, no. 8, Feb. 2022, Art. no. e2106598119.
- [11] D. Zhang, Y. Chen, F. Guo, H. R. Karimi, H. Dong, and Q. Xuan, "A new interpretable learning method for fault diagnosis of rolling bearings," *IEEE Trans. Instrum. Meas.*, vol. 70, 2021, Art. no. 3507010.
- [12] X. Zhao and M. Jia, "A novel unsupervised deep learning network for intelligent fault diagnosis of rotating machinery," *Struct. Health Monitor.*, vol. 19, no. 6, pp. 1745–1763, Nov. 2020.
- [13] W. Zhang, X. Li, and X. Li, "Deep learning-based prognostic approach for lithium-ion batteries with adaptive time-series prediction and on-line validation," *Measurement*, vol. 164, Nov. 2020, Art. no. 108052.
- [14] X. Li and W. Zhang, "Deep learning-based partial domain adaptation method for intelligent machinery fault diagnostics," *IEEE Trans. Ind. Electron.*, vol. 68, no. 5, pp. 4351–4361, May 2021.
- [15] C. He et al., "FedML: A research library and benchmark for federated machine learning," 2020, *arXiv:2007.13518*.

- [16] S. Lu, Z. Gao, Q. Xu, C. Jiang, A. Zhang, and X. Wang, "Class-imbalance privacy-preserving federated learning for decentralized fault diagnosis with biometric authentication," *IEEE Trans. Ind. Informat.*, vol. 18, no. 12, pp. 9101–9111, Dec. 2022.
- [17] W. Zhang, X. Li, H. Ma, Z. Luo, and X. Li, "Federated learning for machinery fault diagnosis with dynamic validation and self-supervision," *Knowl. Based Syst.*, vol. 213, Feb. 2021, Art. no. 106679.
- [18] Q. Liu et al., "Asynchronous decentralized federated learning for collaborative fault diagnosis of PV stations," *IEEE Trans. Netw. Sci. Eng.*, vol. 9, no. 3, pp. 1680–1696, May 2022.
- [19] Z. Zhang, X. Xu, W. Gong, Y. Chen, and H. Gao, "Efficient federated convolutional neural network with information fusion for rolling bearing fault diagnosis," *Control Eng. Pract.*, vol. 116, Nov. 2021, Art. no. 104913.
- [20] X. Ma, C. Wen, and T. Wen, "An asynchronous and real-time update paradigm of federated learning for fault diagnosis," *IEEE Trans. Ind. Informat.*, vol. 17, no. 12, pp. 8531–8540, Dec. 2021.
- [21] S. Sun, H. Huang, T. Peng, C. Shen, and D. Wang, "A data privacy protection diagnosis framework for multiple machines vibration signals based on a swarm learning algorithm," *IEEE Trans. Instrum. Meas.*, vol. 72, pp. 1–9, 2023.
- [22] A. Krizhevsky, I. Sutskever, and G. E. Hinton, "ImageNet classification with deep convolutional neural networks," *Commun. ACM*, vol. 60, no. 6, pp. 84–90, 2017.
- [23] T. Li et al., "WaveletKernelNet: An interpretable deep neural network for industrial intelligent diagnosis," *IEEE Trans. Syst., Man, Cybern., Syst.*, vol. 52, no. 4, pp. 2302–2312, Apr. 2022.
- [24] W. A. Smith and R. B. Randall, "Rolling element bearing diagnostics using the Case Western Reserve University data: A benchmark study," *Mech. Syst. Signal Process.*, vols. 64–65, pp. 100–131, Dec. 2015.
- [25] W. Zhang and X. Li, "Federated transfer learning for intelligent fault diagnostics using deep adversarial networks with data privacy," *IEEE/ASME Trans. Mechatronics*, vol. 27, no. 1, pp. 430–439, Feb. 2022.



**Shilong Sun** (Member, IEEE) received the Ph.D. degree from the City University of Hong Kong, Hong Kong, in 2018.

He is currently an Assistant Professor with the Harbin Institute of Technology, Shenzhen, China. His research interests include vibration energy harvesting design, fault diagnosis and prognosis, decision-making with artificial intelligence, and deep learning for industrial data. Now, he focuses on the remaining equipment life estimation research with deep learning and smart energy harvesting techniques.



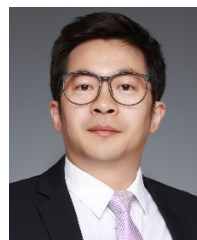
**Haodong Huang** was born in Jingmen, China. He received the B.S. degree in mechanical engineering from the School of Mechanical Engineering and Automation, Northeast Normal University, Changchun, China, in 2021. He is currently pursuing the M.S. degree in mechanical engineering with the School of Mechanical Engineering and Automation, Harbin Institute of Technology, Shenzhen, China.

His research interests include mechanical fault diagnosis and condition monitoring.



**Tengyi Peng** was born in Shaoguan, China. He received the B.S. degree in mechanical design manufacture and automation from the School of Mechanical and Electrical Engineering, University of Electronic Science and Technology of China, Chengdu, China, in 2020. He is currently pursuing the M.S. degree in mechanical engineering with the School of Mechanical Engineering and Automation, Harbin Institute of Technology, Shenzhen, China.

His research interests include mechanical fault diagnosis and condition monitoring.



**Dong Wang** (Member, IEEE) received the Ph.D. degree from the City University of Hong Kong, Hong Kong, in 2015.

He was a Senior Research Assistant, a Post-Doctoral Fellow, and a Research Fellow with the City University of Hong Kong. He is currently an Associate Professor with the Department of Industrial Engineering and Management, Shanghai Jiao Tong University, Shanghai, China, where he is also with the State Key Laboratory of Mechanical System and Vibration. His research interests include sparse and complex measures, signal processing, prognostics and health management, condition monitoring and fault diagnosis, statistical learning and machine learning, statistical process control, and nondestructive testing.

Dr. Wang is an Editorial Board Member of the Mechanical Systems and Signal Processing. He is also an Associate Editor of the IEEE TRANSACTIONS ON INSTRUMENTATION AND MEASUREMENT, Measurement, IEEE SENSORS JOURNAL, and Journal of Dynamics Monitoring and Diagnostics.